

# Meta-LoRA: Meta-Learning LoRA Components for Domain-Aware ID Personalization

Bariş Batuhan Topal  
Pixery Labs  
İstanbul, Türkiye

barisbatuhantopal@gmail.com

Zafer Doğan Budak  
METU Dept. of Electrical and Elec. Engineering  
Ankara, Türkiye  
zafer.budak@metu.edu.tr

Umut Özyurt  
METU Dept. of Computer Engineering  
Ankara, Türkiye

umut.ozyurt@metu.edu.tr

Ramazan Gokberk Cinbis  
METU Dept. of Computer Engineering  
Ankara, Türkiye  
gcinbis@metu.edu.tr

## Abstract

Recent advancements in text-to-image generative models, particularly latent diffusion models (LDMs), have demonstrated remarkable capabilities in synthesizing high-quality images from textual prompts. However, achieving identity personalization—ensuring that a model consistently generates subject-specific outputs from limited reference images—remains a fundamental challenge. To address this, we introduce Meta-Low-Rank Adaptation (Meta-LoRA), a novel framework that leverages meta-learning to encode domain-specific priors into LoRA-based identity personalization. Our method introduces a structured three-layer LoRA architecture that separates identity-agnostic knowledge from identity-specific adaptation. In the first stage, the LoRA Meta-Down layers are meta-trained across multiple subjects, learning a shared manifold that captures general identity-related features. In the second stage, only the LoRA-Mid and LoRA-Up layers are optimized to specialize on a given subject, significantly reducing adaptation time while improving identity fidelity. To evaluate our approach, we introduce Meta-PHD, a new benchmark dataset for identity personalization, and compare Meta-LoRA against state-of-the-art methods. Our results demonstrate that Meta-LoRA achieves superior identity retention, computational efficiency, and adaptability across diverse identity conditions. Our code, model weights, and dataset are released on [barisbatuhan.github.io/Meta-LoRA](https://barisbatuhan.github.io/Meta-LoRA).

## 1. Introduction

Text-to-image generative models have seen significant advancements in recent years, demonstrating a remarkable

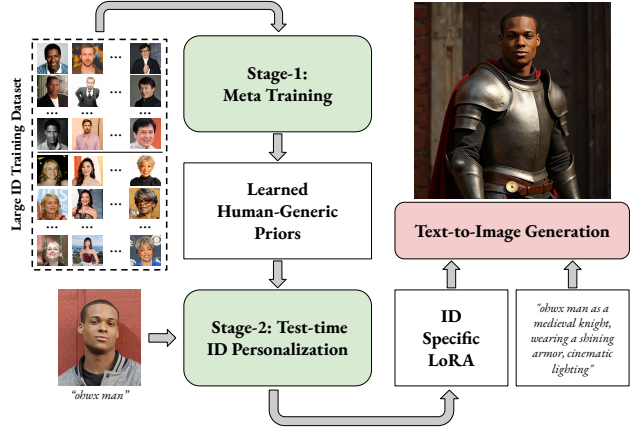


Figure 1. Our overall training and inference pipeline. In the first stage (meta-learning), we learn a subset of LoRA components capturing domain-specific priors, shared across the identities. In the second stage (personalization), only the identity-specific LoRA components are fit from a single image.

ability to generate high-quality images from textual prompt encodings [22]. Among them, latent diffusion models (LDMs) [15, 21, 23, 28] have proven to be particularly effective, utilizing deep learning to iteratively refine images within a latent space. However, achieving identity personalization—generating images that accurately capture a specific subject’s likeness while maintaining generalization— from a single or few image(s) remains a significant challenge [36].

The mainstream approaches to generative model personalization fall broadly into two extremes. On the one end, methods such as DreamBooth [24] and textual inversion [6] rely on general-purpose fine-tuning algorithms for personalization purposes. While effective in many scenarios, these

methods rely purely on the priors embedded into the pre-trained generative model. Such priors, however, often provide insufficient specialization for capturing subtle domain-specific nuances, such as fine facial details. To overcome such limitations, it is commonly necessary to use a rich set of subject examples and update significant portions of model parameters in order to achieve accurate identity adaptation. Parameter-efficient fine-tuning techniques, e.g. Low-Rank Adaptation (LoRA) [10] and its variants [1, 8, 12, 16, 35], attempt to reduce adaptation complexity by constraining parameter updates through carefully designed structures; however, since these are general fine-tuning techniques, they share many of the limitations of the traditional fine-tuning techniques.

At the other extreme, feed-forward conditioning-based approaches [9, 17, 20, 30, 31, 33] train ControlNet-like [34] mechanisms to adapt generative models on-the-fly, circumventing the need for iterative fine-tuning at test time. Although appealing due to their tuning-free adaptation ability, these methods require large-scale training datasets and complex conditioning networks. In addition, their purely feed-forward structure practically limits their ability to capture fine-grained identity details.

In our work, we aim to combine the advantages of these two paradigms, blending the capability of learning domain-specific personalization priors without relying solely on computationally demanding feed-forward conditioning modules. To our knowledge, the only work that closely aligns with this direction is HyperDreamBooth [25]. HyperDreamBooth introduces a hyper-network architecture trained to predict identity-specific LoRA weights from input images, which can then be fine-tuned. However, this design necessitates a large meta-model to map input images to all per-layer LoRA components, inheriting similar drawbacks to pure feed-forward conditioning models: susceptibility to overfitting and challenging training requirements.

To overcome the limitations discussed above, we propose Meta-Low-Rank Adaptation (Meta-LoRA), a novel framework that significantly enhances LoRA-based identity personalization in text-to-image generative models, while maintaining simplicity. Specifically, we propose a structured meta-learning strategy to pre-train a subset of LoRA components in a subject-independent manner, effectively encoding domain-specific priors. This results in a compact, ready-to-adapt LoRA structure that facilitates efficient and precise adaptation to novel identities; avoiding high-complexity modules transforming images to adaptation layers used in prior work [9, 17, 20, 30, 33]. Since our meta-learning yields low-complexity LoRA components, it substantially reduces the required training dataset size compared to prior conditioning-based approaches. Furthermore, the final personalization stage involves a straightforward fine-tuning mechanism that naturally supports a variety of customiza-

tions, such as augmentations and using additional losses.

Our method introduces two key innovations compared to conventional LoRA strategies. First, Meta-LoRA employs a three-layer LoRA architecture, designed specifically to facilitate effective manifold learning of the identity domain. The *LoRA Meta-Down* layer is trained to project inputs onto a domain-specific manifold within the generative model’s feature space, capturing generic identity features shared across individuals. This learned manifold then serves as a foundation for efficiently specializing the subsequent *LoRA Mid* and *LoRA Up* layers to individual identities. Second, we adopt a structured two-stage training pipeline: initially, the Meta-Down layer is meta-trained using multiple identities to encode robust domain-specific priors, effectively establishing a generalized feature representation. Subsequently, for a given target identity, we fine-tune only the compact LoRA Mid and LoRA Up layers using only a single (or a small set of) example image(s), resulting in rapid and accurate personalization. This approach not only improves identity preservation and adaptability but also significantly reduces computational complexity and the amount of data required for personalization. An overview is given in Figure 1.

We evaluate the proposed approach with a focus on the FLUX.1-dev model [15], a state-of-the-art text-to-image diffusion system known for its high image quality and strong prompt adherence. Following prior studies, we assess personalized models trained with Meta-LoRA based on (i) the retention of the base model’s original capabilities and (ii) the fidelity of generated faces to target identities. However, our analysis highlights inconsistencies in recent literature regarding dataset choices and evaluation protocols, particularly the problematic reuse of the same image for both personalization and evaluation, which inflates performance estimates. To address these issues, we introduce Meta-PHD, a robust benchmark featuring diverse identities across multiple sources, with varied poses, lighting, and backgrounds, ensuring a rigorous evaluation of identity personalization methods. Our qualitative analysis further complements the quantitative results, capturing subtle yet significant details that conventional metrics may overlook. Together, our results demonstrate that the proposed approach not only preserves identity across diverse scenarios but also maintains strong generalization and prompt adherence, highlighting the potential of meta-learning for enhancing LoRA-based identity personalization.

In summary, our contributions are: (1) a novel Meta-LoRA architecture that separates generic and identity-specific components, (2) a meta-learning strategy, and an effective optimization algorithm, enabling one-shot personalization, (3) a new benchmark dataset (Meta-PHD) for rigorous evaluation, and (4) a Robust Face Similarity metric to better measure identity retention.

## 2. Related Works

Identity personalization methods can be grouped into two: fine-tuning and feed-forward conditioning based approaches. In a pioneering work, Ruiz et al. [24] introduces DreamBooth, a fine-tuning approach that balances training with a class-specific prior-preservation loss to maintain model generalization. Custom Diffusion [13] fine-tunes select cross-attention parameters for integrating novel concepts. LoRA [10] offers a parameter-efficient alternative to fine-tuning parameters directly, enabling controlled adaptation by introducing low-rank updates to the model weights. Given its widespread adoption, we focus on the original LoRA formulation, though Meta-LoRA can naturally extend to other LoRA variants, e.g. [1, 8, 12, 16, 35].

In the second group of methods, several feed-forward conditioning methods have recently been proposed (see [36] for a recent survey). For example, PortraitBooth [20], PhotoMaker [17], InstantBooth [27], PhotoVerse [3], FastComposer [32], InstantID [30], and PuLID [9] all incorporate an IP-Adapter-like design, leveraging identity-related embeddings extracted from input ID images to manipulate text-conditioned generation with various enhancements: PortraitBooth and PhotoMaker fine-tune the diffusion model, with PortraitBooth further introducing an identity loss and locational cross-attention control. InstantBooth integrates an adapter layer positioned after the cross-attention mechanism to inject conditional features into U-Net layers. InstantID employs a ControlNet module that incorporates facial landmarks and identity embeddings. FastComposer incorporates subject embeddings extracted from an image encoder in order to augment the generic text conditioning in diffusion models. In PhotoVerse, a dual-branch conditioning mechanism operates across both text and image domains, while the training is further reinforced by a facial identity loss. PuLID enhances identity preservation through ID loss and improves text-image alignment via an alignment loss. In contrast to these works, Meta-LoRA does not require training a complex conditioning model. In addition, we simply use only diffusion loss; although the incorporation of additional losses is an orthogonal direction, and can easily be incorporated into the Meta-LoRA training, if desired.

As a work mixing elements from both groups of personalization approaches, HyperDreamBooth [25] adopts a two-stage pipeline: first, a meta-module is trained to generate LoRA-like weights based on an identity image; second, these generated weights undergo fine-tuning for the specific identity. While this method aligns with our work to some extent, it introduces several limitations that hinder its scalability and applicability; as it requires training of a complex image-to-LoRAs mapping network, expressed by a recurrent transformer architecture. In contrast, we propose to simply meta-learn a subset of LoRA components to embed domain-specific priors.

Finally, we should note that our work has been inspired by the prior work on meta-learning for classification and reinforcement learning tasks. We similarly embrace the meta-learning for fast-adaptation idea pioneered by MAML [5]. The formulation and technical details of Meta-LoRA, however, are vastly different virtually in all major ways.

## 3. Methodology

In this section, we provide a detailed explanation of Meta-LoRA, including the model structure and an efficient training algorithm.

### 3.1. Preliminaries on Text-to-Image LoRA Training

In diffusion-based text-to-image (T2I) models, Low-Rank Adaptation (LoRA) [10] is primarily integrated into the attention mechanisms of the U-Net backbone, particularly within the cross-attention layers that facilitate interactions between latent image representations and text embeddings. By incorporating low-rank decomposition matrices into the weight update process, LoRA enables efficient fine-tuning while minimizing modifications to the original model parameters. In more advanced architectures, such as Stable Diffusion XL [21] and FLUX.1 [15], LoRA may also be applied to transformer-based components, enhancing latent feature extraction and improving T2I coherence. By limiting adaptation to these critical layers, LoRA optimizes parameter efficiency while maintaining the integrity of the underlying diffusion model.

We integrate our Meta-LoRA architecture into FLUX.1-dev, a state-of-the-art T2I generation model. However, the Meta-LoRA design follows a generic approach, making it adaptable to other models with similar architectures.

### 3.2. Meta-LoRA Architecture

We propose a three-layer adaptation framework by redefining the original LoRA Down-block as an identity-shared adaptation component, which we call LoRA Meta-Down (LoMD), and decomposing the conventional LoRA Up-block into two sub-components, which we call LoRA Mid (LoM) and LoRA Up (LoU). Specifically, given some pre-trained linear layer  $W_0 : \mathcal{R}^{d_1} \rightarrow \mathcal{R}^{d_2}$  and its input  $x$ , Meta-LoRA applies the following residual update:

$$h = W_0 x + \Delta W x \quad (1)$$

$$= W_0 x + L_{\text{up}}^i L_{\text{mid}}^i L_{\text{meta-down}} x \quad (2)$$

where  $L_{\text{meta-down}}$ ,  $L_{\text{mid}}^i$ , and  $L_{\text{up}}^i$  correspond to LoMD, LoM and LoU, respectively. The index  $i \in \{1, \dots, N\}$  indicates the identity among  $N$  training identities.

Each LoMD component serves as an identity-independent module shared across all identities to model the personalization manifold for the targeted domain (Figure 2, left). Once

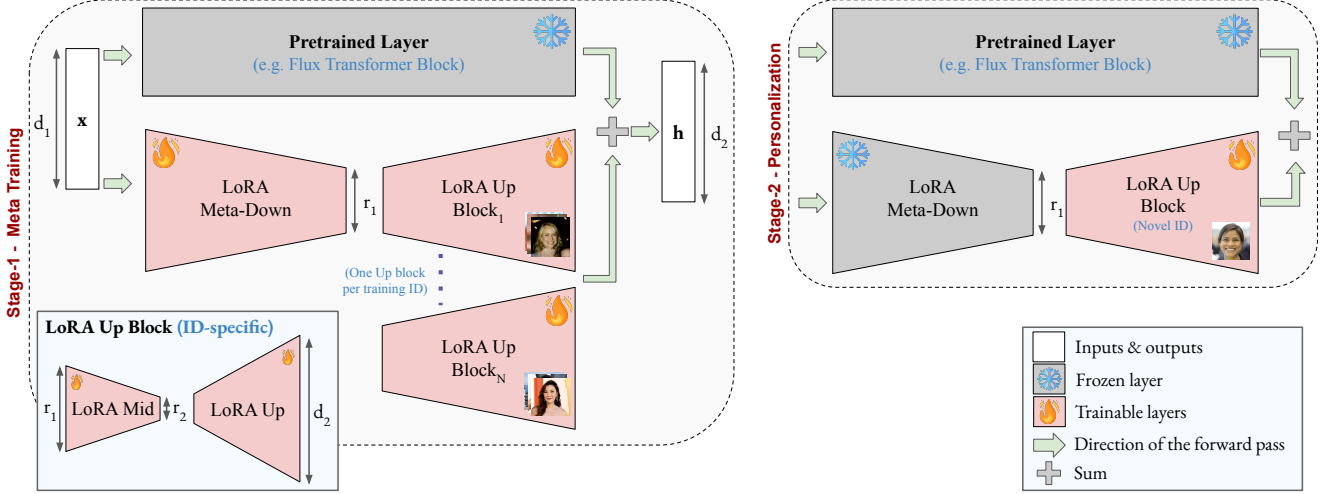


Figure 2. Proposed Meta-LoRA architecture. LoRA Meta-Down components correspond to the identity-independent LoRA components providing the domain priors into the LoRA structure. LoRA Up Blocks are defined in an identity-specific manner. During meta-training (Stage 1), the LoRA Meta-Down components are trained, along with the temporary LoRA Up Blocks corresponding to the training IDs. During testing, for a novel ID, a new set of LoRA Up Blocks are initialized and trained, while LoRA Meta-Down layers are kept frozen.

trained, LoMD remains frozen during test-time personalization, acting as a learned prior that facilitates rapid adaptation (Figure 2, right). The second and third components, LoM and LoU, are identity-specific, and therefore, parameterized separately for each identity. LoM reduces the output dimension of LoMD from  $r_1$  to a lower-rank representation  $r_2$ , improving efficiency while retaining relevant features, whereas LoU transforms this reduced representation back to the same dimensionality ( $d_2$ ) as the output of the pre-trained layer  $W_0$ , ensuring compatibility with the base model.

### 3.3. Training

Our training pipeline comprises two main stages: meta-training and test-time ID personalization. During meta-training, we learn a shared LoRA Meta-Down (LoMD) module for general features while employing distinct LoRA Mid (LoM) and LoRA Up (LoU) layers for character-specific details. In the test-time personalization stage, we fine-tune the LoM and LoU layers based on the given identity image. The following subsections provide a detailed explanation of each stage.

#### 3.3.1. Stage-1: Meta-Training

The key challenge in the meta-training stage is learning a robust meta-representation in LoMD, while preventing under- or overfitting in the identity-specific LoM and LoU layers. A simple training approach could be optimizing all LoRA components simultaneously, for all characters. However, it is not possible to construct batches large enough to cover all identities. Trying to naively remedy this problem by applying stochastic gradient descent to the LoM and LoU components of only the identities available in each batch

(and the shared LoMD parameters) also yields poor training efficiency, since the identity-specific parameters are updated much less frequently than the shared ones, resulting in poor gradients for LoMD updates.

To achieve efficient training with small batch sizes, we divide the dataset into buckets, each containing a subset of training identities. To minimize the I/O overhead, we make model updates for  $q_{\text{bucket}}$ -many iterations using each bucket data. We note that buckets can contain data larger than the maximum batch size that the VRAM allows.

Importantly, at the beginning of a new bucket, we first apply an adaptive *warm-up procedure*: in the first  $q_{\text{warm-up}}$  iterations of a new bucket, only the LoM and LoU layers corresponding to the bucket contents are updated, syncing them with the current status of the LoMD components.

In practice, we set  $q_{\text{bucket}}$  such that each example in a bucket is utilized for 10 iterations. We set  $q_{\text{warm-up}} = 0.4 \cdot q_{\text{bucket}}$  empirically to ensure that LoMD is updated only after the character-specific layers have sufficiently adapted. In the remaining iterations, LoMD is refined using more informative gradients, ensuring that the learned meta-representation continues to improve without being biased by individual identities. For all model updates, we simply use the latent-space diffusion loss  $\mathcal{L}_{\text{diff}}$ .

This structured approach prevents poor generalization due to under-trained identity-specific layers, while also mitigating the risk of overfitting. Throughout the meta-training stage, LoMD modules accumulate the common domain knowledge from which all individual-specific personalized models are expressed. At the end of this phase, all trained LoM and LoU components are discarded, and only LoMD



components are retained.

### 3.3.2. Stage-2: Test-time ID Personalization

In the second stage, we train only the LoM and LoU layers using a novel target identity image, while keeping the LoMD weights frozen. The  $r_1$  dimension (i.e., the LoMD output dimension) remains unchanged, whereas  $r_2$  (i.e., the LoM output dimension) is set to 1 to mitigate overfitting due to the single-image input.

Although our focus is one-shot personalization, Meta-LoRA naturally extends to settings with multiple reference images. In such cases, the  $r_2$  dimension can be increased to enhance model capacity, potentially improving identity fidelity - a promising direction for future exploration. Finally, for simplicity, the final model can be converted back into the default LoRA structure by multiplying the LoMD and LoM matrices, producing a rank- $r_2$  (rank-1 in our experiments) LoRA model. All results presented in this paper are obtained using this conversion.

To further prevent overfitting on a single image, we apply data augmentations. First, we detect the face in the image and determine the longer side length of the facial bounding box ( $f_{long}$ ). Then, we create multiple crops of the image using common aspect ratios: 16:9, 4:3, 1:1, 3:4, and 9:16. For each aspect ratio, we center the face and set the shorter side of the cropped image to one of the following values:  $f_{long} \cdot \{1.5, 2, 2.5, 3.5, 4.5\}$ . If the original image does not support a specific crop size, we select the closest possible size if an image with that size is not extracted. Additionally, we apply random horizontal flips to each image. In total, we generate at most 25 augmented images from a single input.

## 4. Experiments

In this section, we evaluate the performance of our approach both quantitatively and qualitatively in comparison to state-of-the-art text-to-image personalization methods. We first introduce our evaluation dataset, experimental setup, and metrics, then present comparative results and discussions.

### 4.1. Benchmark data set

To rigorously assess personalization performance, we curated a new test dataset, termed the **Meta-LoRA Personalization of Humans Dataset (Meta-PHD)**. This dataset comprises two complementary parts—drawn from FFHQ [11] and Unsplash-50 [7]—and includes both image and prompt collections designed to challenge the model’s ability to preserve identity and adhere to diverse textual prompts. We will make the Meta-PHD dataset publicly available to facilitate fair comparisons.

**Meta-PHD-FFHQ images.** The Meta-PHD-FFHQ component contains 60 high-quality face images (30 male and 30 female) selected from the FFHQ test set [11]. These images cover a diverse range of ages and skin tones to ensure broad

applicability. We applied strict selection criteria to each image: only one individual is present, the face is unobstructed (i.e., no sunglasses, hats, or hands), the eyes are open, and the head is oriented within 30 degrees of frontal.

**Meta-PHD-Unsplash images.** This component is inspired by the Unsplash-50 dataset [7] and is sourced from <https://unsplash.com/> under permissive licenses. It comprises 98 images collected from 16 identities (with 4–10 images per identity). Within each identity, subjects appear in consistent attire and backgrounds but exhibit varied poses. This design ensures the dataset captures a range of views, thus preventing models from succeeding by merely replicating a single reference pose.

**Prompts.** For the FFHQ component, we prepared 20 prompts per gender (with some overlap) to test the model’s ability to generate both stylistic transformations and re-contextualizations. These prompts, inspired by prior work [9, 25, 27, 30, 33], evaluate both prompt adherence and identity preservation. For the Unsplash component, we designed 10 prompts per identity focusing on pose and background variations while enforcing a frontal, unobstructed view of the subject. An example prompt is: *“A man/woman standing in a sunlit urban plaza, facing directly toward the camera with a fully detailed face and direct eye contact”*. The complete prompt list is shared in the Supplementary Material.

### 4.2. Experimental setup

**Training dataset.** We utilize a proprietary data set of male and female images with distinct identities from those in the test benchmark and train two separate models. Each individual is represented by 20 high-resolution images ( $> 720p$ ). The dataset includes 1,050 female and 400 male subjects. The dataset is diverse in terms of age, skin tone, image environments, and accessories.

**Implementation details.** We trained the Stage-1 Meta-LoRA model for 50,000 iterations, on a single A6000 GPU. For Stage-2 training, we use 375 iterations. These values are decided empirically. Additional implementation details can be found in the Supplementary Material. The code, model weights, and the evaluation dataset will be shared publicly.

**Baseline models.** We compare against three state-of-the-art subject-driven image generation models: InstantID [30], PhotoMaker [17], and PuLID [9]. For fairness, we align evaluation conditions where possible. Additionally, we provide comparisons against a standard rank-1 LoRA baseline, both with and without augmented training data, trained for the same number of iterations (375) as Meta-LoRA, as well as longer (675). A more detailed explanation of the baselines, including the rationale behind various details such as diffusion backbones, is given in the Supplementary Material.

Model	Base Model	Train Dataset	CLIP-T (%) $\uparrow$	CLIP-I (%) $\uparrow$	DINO (%) $\uparrow$	R-FaceSim (%) $\uparrow$
InstantID [30]	SD-XL [21]	60M	29.37	65.17	53.24	72.09
	SD-XL Lightning [18]		30.52	70.79	60.34	75.26
	RealVisXL V4 [26]		30.53	70.07	65.17	73.77
PhotoMaker [17]	SD-XL	112K	31.51	73.55	68.35	67.57
	SD-XL Lightning		<u>31.92</u>	78.28	76.82	63.51
	RealVisXL V4		31.64	74.14	77.58	69.14
PuLID [9]	SD-XL	1.5M	31.12	69.83	63.53	71.06
	SD-XL Lightning		31.86	77.91	73.53	73.50
	RealVisXL V4		31.12	73.79	74.67	75.19
	FLUX.1-dev [15]		30.95	74.66	74.01	75.72
Rank-1 LoRA 375 Iters [10] + augmented inputs	FLUX.1-dev	0	<b>31.95</b>	<b>81.96</b>	<u>80.01</u>	57.62
	FLUX.1-dev		31.88	80.42	<b>80.25</b>	72.69
Rank-1 LoRA 625 Iters + augmented inputs	FLUX.1-dev		31.63	79.48	77.81	61.41
	FLUX.1-dev		31.47	77.21	77.33	<u>76.15</u>
Meta-LoRA (ours)	FLUX.1-dev	8K (male), 21K (female)	31.66	77.96	77.55	<b>77.16</b>

Table 1. Quantitative comparison of our model with the state-of-the-art publicly available studies in the literature. The scores are taken for five seeds and for both male and female subsets, and averaged to reach the final output. While CLIP-T, CLIP-I and DINO are calculated from the Meta-PHD-FFHQ subset, R-FaceSim is computed using the Meta-PHD-Unsplash images.

### 4.3. Evaluation metrics and R-FaceSim

Following recent studies [9, 24, 25, 27, 30, 33], we use four key metrics to evaluate performance: *CLIP-T*, *CLIP-I*, *DINO*, and the newly proposed *Robust Face Similarity (R-FaceSim)*. The details of the first three metrics are given in the Supplementary Material. The commonly used FaceSim metric aims to evaluate how well the generated images maintain the subject’s identity based on the cosine similarity between the reference and generated images. The facial embeddings are obtained using the backbone of a face recognition model. However, we observe two major limitations with it. First, facial recognition methods primarily learn to distinguish individuals, therefore, their embeddings rather tend to lack some of the fine-grained identity details, also observed by [4, 14, 25] in various contexts. Second, commonly the same reference images are used for both personalization and face similarity evaluation. However, in feed-forward personalization models, e.g. InstantID [30] and PuLID [9], we observe a bias towards generating images with the same pose and/or gaze as the reference images. This phenomenon indicates an undesirable limitation of those models. It also tends to artificially inflate the face-similarity scores, because the face recognition embeddings are sensitive to having the same pose or gaze.

To address the former issue, we provide a detailed discussion of the qualitative results. To address the latter one, we propose a novel face-similarity metric that we call *Robust Face Similarity (R-FaceSim)*. R-FaceSim is computed by excluding the reference image (used for fine-tuning or output-conditioning); we instead compare each generated image to other real images of the same person (with different poses) and average the cosine similarity. This yields a face-similarity score not inflated by the exact reference image. We

encourage future research to adopt this approach to improve the inflated scores from pose copying as acknowledged in [7].

### 4.4. Quantitative Results

Table 1 provides a quantitative comparison of Meta-LoRA against the previously mentioned baselines on the Meta-PHD test set. Our evaluation focuses on three key aspects: CLIP-T, CLIP-I, and DINO scores, which assess prompt adherence and visual alignment; R-FaceSim, which measures identity preservation; and the size of the training datasets.

Due to the nature of CLIP-I and DINO, models that generate images closely resembling their base model tend to achieve higher scores in these metrics. However, strong generalization capabilities in base models can result in lower CLIP-T scores when fine-tuned for identity personalization. Meanwhile, R-FaceSim increases when the reference identity is overfitted, but excessive training can degrade generalization. Existing identity personalization models struggle to balance these competing objectives. InstantID [30] and PhotoMaker [17], for instance, show a bias toward either face similarity or text/image alignment. PhotoMaker exhibits higher CLIP-T, CLIP-I, and DINO scores at the cost of identity preservation, whereas InstantID prioritizes facial similarity at the expense of generalization. PuLID [9] and our proposed Meta-LoRA, on the other hand, achieve a better balance between identity preservation and generalization.

Compared to InstantID, our model outperforms across all evaluation metrics, achieving a more balanced trade-off between prompt adherence and identity retention. Against PhotoMaker, Meta-LoRA delivers comparable results in CLIP-I, CLIP-T, and DINO metrics while exhibiting superior facial similarity. Additionally, when compared to PuLID with the FLUX.1-dev [15] base, Meta-LoRA maintains better face

similarity (i.e., a higher R-FaceSim score) while exhibiting superior prompt-following ability and a stronger capacity to inject identity-specific details without distorting the overall scene (i.e., higher CLIP-T, CLIP-I, and DINO scores). Given that both models share an implementation with the same base module, we find it most logical to compare Meta-LoRA with PuLID using the FLUX.1-dev [15] variation. However, similar observations hold for other PuLID variations as well.

Another key distinction lies in the amount of pretraining data and the additional training losses employed. Existing models rely on significantly larger datasets (i.e., our dataset is 0.035% of InstantID, 1.4% of PuLID, and 18.75% of PhotoMaker). Additionally, PuLID incorporate a face-centric ID loss during training and InstantID integrates facial features to its network. Despite this, Meta-LoRA achieves competitive or superior results without the use of such explicit facial losses or features, opting instead for a simpler and more efficient training strategy.

We also evaluate default Rank-1 LoRA models trained with direct and augmented inputs. At 375 iterations, these models achieve high CLIP and DINO scores but exhibit low face similarity, indicating under-fitting. In contrast, Meta-LoRA converges faster, achieving a well-balanced state at 375 iterations. Extending Rank-1 LoRA training to 625 iterations stabilizes the model if the input is augmented, yet Meta-LoRA still outperforms Rank-1 LoRA (625 iterations, plus data augmentations) across all evaluation metrics, demonstrating its efficiency and effectiveness. A more detailed comparison is given in the Supplementary Material.

#### 4.5. Qualitative Results

To evaluate the visual fidelity and prompt adherence of Meta-LoRA, we conduct a qualitative comparison against several baseline methods [9, 10, 17, 30]. To enhance the rigor of our qualitative assessment of visual outcomes, we focus our presentation on female samples. This decision is predicated on the fact that Stage-1 training incorporated a larger dataset of female subjects. A more exhaustive comparative analysis of male subjects, encompassing a broader spectrum of identities, textual prompts, and base model outputs, is available in the Supplementary Material.

Figure 3 presents a qualitative comparison of different models, where each column corresponds to a specific input identity, with the reference image displayed in the first row. The subsequent rows showcase outputs generated by each method under the same prompt. Our analysis highlights key differences in identity preservation, prompt adherence, and overall image quality. First of all, **Meta-LoRA** demonstrates the strongest ability to maintain facial characteristics while accurately integrating the details of the given prompt. Unlike other methods, it effectively balances identity retention with scene coherence, producing visually faithful results that align well with textual descriptions. The generated images



Figure 3. Qualitative comparisons. Meta-LoRA shows better ID preservation while keeping prompt alignment. Meta-LoRA keeps the pose natural (1st column), promotes identities effectively (2nd and 3rd columns), and follows the given style (4th column). Details are best viewed on screen, zoomed-in.

exhibit both high visual fidelity and strong textual alignment, making Meta-LoRA the most robust approach across diverse scenarios.

In contrast, **LoRA** shows success in following textual prompts but struggles with preserving identity, leading to inconsistencies in facial features. **InstantID**, on the other hand, exhibits a strong replication of pose and composition of the reference image. While this allows generated images to be more physically consistent for a subset of prompts, it significantly compromises the model’s ability to adhere to prompts that specify different poses, viewpoints, or artistic styles requiring a change in facial geometry. This behavior explains the artificially inflated identity similarity scores under naive evaluation metrics, contrasted with its weaker performance under metrics that prioritize prompt alignment.



**PhotoMaker** demonstrates a reasonable ability to capture the general appearance of the subject. However, it frequently struggles to reproduce fine-grained facial details, particularly when the prompt necessitates significant alterations in context or style. Meanwhile, **PuLID** achieves comparable facial similarity to Meta-LoRA but tends to "correct" or smooth out distinctive identity cues that conventional face similarity metrics may not fully capture [4]. In contrast, Meta-LoRA inherits and propagates these fine details, ensuring a more faithful representation of the reference identity. Additionally, Meta-LoRA exhibits superior prompt adherence, generating images with richer contextual elements, more detailed backgrounds, and an overall enhanced sense of naturalness.



Figure 4. Qualitative comparisons across different seeds. For each different seed, Meta-LoRA successfully generates distinct variations, while also preserving the prompt alignment. Details are best viewed on screen, zoomed-in.

Figure 4 further examines the impact of random seed variation on the generated outputs. Each column presents images generated using the same seed for LoRA, PuLID, and Meta-LoRA, allowing for a direct comparison of their consistency and adaptability. This comparison also reveals several key insights: while **LoRA** produces outputs that often share similarities in pose and background with those of Meta-LoRA, it tends to overfit to background elements unrelated to the target identity. This results in spurious correlations, suggesting that the model is learning incidental features from

the reference image rather than focusing exclusively on core identity characteristics.

**PuLID** exhibits a relatively low degree of variation across different seeds, suggesting a potential limitation in its ability to explore the full range of possible outputs consistent with the prompt and identity. Its prompt following capabilities also fall short in some cases in terms of modifying facial features according to the prompt.

In contrast, **Meta-LoRA** achieves a desirable balance between seed-dependent variation and identity consistency. It generates diverse outputs while maintaining a high degree of fidelity to the input identity, ensuring both adaptability and accuracy across different scenarios.

Overall, the qualitative results strongly corroborate our quantitative findings. Meta-LoRA consistently produces identity-accurate images across a wide range of prompts, preserving the subject’s distinctive facial features while generating scenes that closely align with textual descriptions. Additionally, it maintains meaningful variation across different seeds, offering both creativity and faithfulness—an improvement that is particularly valuable in applications requiring both identity preservation and prompt adherence.

## 5. Conclusion

In this paper, we present Meta-Low-Rank Adaptation (Meta-LoRA), a versatile three-layer LoRA architecture designed to enhance identity personalization in text-to-image generative models. Meta-LoRA employs a two-stage training strategy: the first stage learns generic LoRA Meta-Down layers applicable across multiple identities, while the second stage fine-tunes the LoRA Mid and LoRA Up layers for a specific identity using only a single reference image. By integrating domain-specific priors and optimizing feature learning across diverse identities, Meta-LoRA significantly improves identity preservation, robustness, and adaptability—all while maintaining computational efficiency.

To evaluate our approach, we introduce Meta-PHD, a novel identity personalization dataset used exclusively for testing, and assess Meta-LoRA’s performance using this dataset. Our results demonstrate that Meta-LoRA achieves state-of-the-art (SOTA) performance or performs comparably to existing SOTA methods. Moreover, qualitative evaluations highlight Meta-LoRA’s ability to generate identity-personalized images while effectively maintaining prompt adherence.

Future research directions include the incorporation of recent LoRA variants [1, 8, 12, 16, 35] into the Meta-LoRA framework and the exploration of the proposed method’s applicability to other model customization tasks.



## Acknowledgments

This work was supported in part by the METU Research Fund Project ADEP-312-2024-11525 and BAGEP Award of the Science Academy. The numerical calculations reported in this paper were partially performed using the MareNostrum 5 pre-exascale supercomputing system. We gratefully acknowledge the Barcelona Supercomputing Center (BSC) and the Scientific and Technological Research Council of Turkey (TÜBİTAK) for providing access to these resources and supporting this research. We also gratefully acknowledge the computational resources kindly provided by METU ImageLab and METU ROMER.

## References

- [1] Shubhankar Borse, Shreya Kadambi, Nilesh Pandey, Kartikeya Bhardwaj, Viswanath Ganapathy, Sweta Priyadarshi, Risheek Garrepalli, Rafael Esteves, Munawar Hayat, and Fatih Porikli. Foura: Fourier low-rank adaptation. In *NeurIPS*, 2024. 2, 3, 8
- [2] Qiong Cao, Li Shen, Weidi Xie, Omkar M Parkhi, and Andrew Zisserman. Vggface2: A dataset for recognising faces across pose and age. In *IEEE Int. Conf. on Automatic Face & Gesture Recognition*, pages 67–74. IEEE, 2018. 11
- [3] Li Chen, Mengyi Zhao, Yiheng Liu, Mingxu Ding, Yangyang Song, Shizun Wang, Xu Wang, Hao Yang, Jing Liu, Kang Du, et al. Photoverse: Tuning-free image customization with text-to-image diffusion models. *arXiv preprint arXiv:2309.05793*, 2023. 3
- [4] Xu Chen, Keke He, Junwei Zhu, Yanhao Ge, Wei Li, and Chengjie Wang. Hifivfs: High fidelity video face swapping. *arXiv preprint arXiv:2411.18293*, 2024. 6, 8
- [5] Chelsea Finn, Pieter Abbeel, and Sergey Levine. Model-agnostic meta-learning for fast adaptation of deep networks. In *ICML*, 2017. 3
- [6] Rinon Gal, Yuval Alaluf, Yuval Atzmon, Or Patashnik, Amit H Bermano, Gal Chechik, and Daniel Cohen-Or. An image is worth one word: Personalizing text-to-image generation using textual inversion. *arXiv preprint arXiv:2208.01618*, 2022. 1
- [7] Rinon Gal, Or Lichter, Elad Richardson, Or Patashnik, Amit H Bermano, Gal Chechik, and Daniel Cohen-Or. Lcm-lookahead for encoder-based text-to-image personalization. In *ECCV*, pages 322–340. Springer, 2024. 5, 6
- [8] Ziqi Gao, Qichao Wang, Aochuan Chen, Zijiang Liu, Bingzhe Wu, Liang Chen, and Jia Li. Parameter-efficient fine-tuning with discrete fourier transform. In *ICML*, 2024. 2, 3, 8
- [9] Zinan Guo, Yanze Wu, Chen Zhuowei, Peng Zhang, Qian He, et al. Pulid: Pure and lightning id customization via contrastive alignment. *NEURIPS*, 37:36777–36804, 2025. 2, 3, 5, 6, 7, 13, 15
- [10] Edward J Hu, Yelong Shen, Phillip Wallis, Zeyuan Allen-Zhu, Yuanzhi Li, Shean Wang, Lu Wang, Weizhu Chen, et al. Lora: Low-rank adaptation of large language models. In *ICLR*, 2022. 2, 3, 6, 7, 15
- [11] Tero Karras. A style-based generator architecture for generative adversarial networks. *arXiv preprint arXiv:1812.04948*, 2019. 5
- [12] Dawid Jan Kopiczko, Tijmen Blankevoort, and Yuki M Asano. Vera: Vector-based random matrix adaptation. In *ICLR*, 2024. 2, 3, 8
- [13] Nupur Kumari, Bingliang Zhang, Richard Zhang, Eli Shechtman, and Jun-Yan Zhu. Multi-concept customization of text-to-image diffusion. In *CVPR*, pages 1931–1941, 2023. 3
- [14] Han-Wei Kung, Tuomas Varanka, Sanjay Saha, Terence Sim, and Nicu Sebe. Face anonymization made simple. *arXiv preprint arXiv:2411.00762*, 2024. 6
- [15] Black Forest Labs. Flux. <https://github.com/black-forest-labs/flux>, 2024. 1, 2, 3, 6, 7, 15
- [16] Yang Li, Shaobo Han, and Shihao Ji. Vb-lora: Extreme parameter efficient fine-tuning with vector banks. In *NEURIPS*, 2024. 2, 3, 8
- [17] Zhen Li, Mingdeng Cao, Xintao Wang, Zhongang Qi, Ming-Ming Cheng, and Ying Shan. Photomaker: Customizing realistic human photos via stacked id embedding. In *CVPR*, pages 8640–8650, 2024. 2, 3, 5, 6, 7, 13, 15
- [18] Shanchuan Lin, Anran Wang, and Xiao Yang. Sdxl-lightning: Progressive adversarial diffusion distillation. *arXiv preprint arXiv:2402.13929*, 2024. 6, 15
- [19] I Loshchilov. Decoupled weight decay regularization. *arXiv preprint arXiv:1711.05101*, 2017. 11
- [20] Xu Peng, Junwei Zhu, Boyuan Jiang, Ying Tai, Donghao Luo, Jiangning Zhang, Wei Lin, Taisong Jin, Chengjie Wang, and Rongrong Ji. Portraitbooth: A versatile portrait model for fast identity-preserved personalization. In *CVPR*, pages 27080–27090, 2024. 2, 3
- [21] Dustin Podell, Zion English, Kyle Lacey, Andreas Blattmann, Tim Dockhorn, Jonas Müller, Joe Penna, and Robin Rombach. Sdxl: Improving latent diffusion models for high-resolution image synthesis. *arXiv preprint arXiv:2307.01952*, 2023. 1, 3, 6, 15
- [22] Alec Radford, Jong Wook Kim, Chris Hallacy, Aditya Ramesh, Gabriel Goh, Sandhini Agarwal, Girish Sastry, Amanda Askell, Pamela Mishkin, Jack Clark, et al. Learning transferable visual models from natural language supervision. In *ICML*, pages 8748–8763. PMLR, 2021. 1, 11
- [23] Robin Rombach, Andreas Blattmann, Dominik Lorenz, Patrick Esser, and Björn Ommer. High-resolution image synthesis with latent diffusion models. In *CVPR*, pages 10684–10695, 2022. 1
- [24] Nataniel Ruiz, Yuanzhen Li, Varun Jampani, Yael Pritch, Michael Rubinstein, and Kfir Aberman. Dreambooth: Fine tuning text-to-image diffusion models for subject-driven generation. In *CVPR*, pages 22500–22510, 2023. 1, 3, 6, 11
- [25] Nataniel Ruiz, Yuanzhen Li, Varun Jampani, Wei Wei, Tingbo Hou, Yael Pritch, Neal Wadhwa, Michael Rubinstein, and Kfir Aberman. Hyperdreambooth: Hypernetworks for fast personalization of text-to-image models. In *CVPR*, 2024. 2, 3, 5, 6
- [26] CivitAI: SG\_161222. Realvisxl v4.0. <https://civitai.com/models/139562?modelVersionId=344487>, 2024. 6, 15

- [27] Jing Shi, Wei Xiong, Zhe Lin, and Hyun Joon Jung. Instantbooth: Personalized text-to-image generation without test-time finetuning. In *CVPR*, 2024. [3](#), [5](#), [6](#)
- [28] Stability AI. Introducing stable diffusion 3.5, 2024. [1](#)
- [29] Christian Szegedy, Sergey Ioffe, Vincent Vanhoucke, and Alexander Alemi. Inception-v4, inception-resnet and the impact of residual connections on learning. In *AAAI*, 2017. [11](#)
- [30] Qixun Wang, Xu Bai, Haofan Wang, Zekui Qin, Anthony Chen, Huaxia Li, Xu Tang, and Yao Hu. Instantid: Zero-shot identity-preserving generation in seconds. *arXiv preprint arXiv:2401.07519*, 2024. [2](#), [3](#), [5](#), [6](#), [7](#), [13](#), [15](#)
- [31] Yuxiang Wei, Yabo Zhang, Zhilong Ji, Jinfeng Bai, Lei Zhang, and Wangmeng Zuo. Elite: Encoding visual concepts into textual embeddings for customized text-to-image generation. In *CVPR*, pages 15943–15953, 2023. [2](#)
- [32] Guangxuan Xiao, Tianwei Yin, William T Freeman, Frédo Durand, and Song Han. Fastcomposer: Tuning-free multi-subject image generation with localized attention. *IJCV*, pages 1–20, 2024. [3](#)
- [33] Hu Ye, Jun Zhang, Sibio Liu, Xiao Han, and Wei Yang. Ip-adapter: Text compatible image prompt adapter for text-to-image diffusion models, 2023. [2](#), [5](#), [6](#)
- [34] Lvmin Zhang, Anyi Rao, and Maneesh Agrawala. Adding conditional control to text-to-image diffusion models. In *CVPR*, pages 3836–3847, 2023. [2](#)
- [35] Qingru Zhang, Minshuo Chen, Alexander Bukharin, Pengcheng He, Yu Cheng, Weizhu Chen, and Tuo Zhao. Adaptive budget allocation for parameter-efficient fine-tuning. In *ICLR*, 2023. [2](#), [3](#), [8](#)
- [36] Xulu Zhang, Xiao-Yong Wei, Wengyu Zhang, Jinlin Wu, Zhaoxiang Zhang, Zhen Lei, and Qing Li. A survey on personalized content synthesis with diffusion models. *arXiv preprint arXiv:2405.05538*, 2024. [1](#), [3](#)

# Meta-LoRA: Meta-Learning LoRA Components for Domain-Aware ID Personalization

## Supplementary Material

### 6. Overview

This document provides various additional details and discussions as an extension of the main Meta-LoRA paper.

### 7. Implementation Details

Meta-LoRA is designed using the ai-toolkit<sup>1</sup> framework. Its training and evaluation are conducted on a single NVIDIA RTX A6000 GPU with 48 GB of VRAM. Under these configurations, Stage-1 training takes approximately 7 days (13 seconds per iteration, 50,000 iterations in total), while Stage-2 training lasts around 18 minutes (2.8 seconds per iteration, 375 iterations in total). For all training runs, we set the learning rate to 0.0004, total number of stage-1 iterations ( $q_{total}$ ) to 50,000,  $q_{bucket}$  to 2,500,  $q_{warm-up}$  to 1,000, and total number of stage-2 iterations ( $q_{st2}$ ) to 375. The batch sizes are selected as 4 and 1 in Stage-1 and Stage-2, respectively. Our model is trained using the default L2-loss and AdamW [19] is preferred as the optimizer.

### 8. Meta-training and Personalization Algorithms

In this subsection, we give the algorithms for the proposed meta-training and test-time ID personalization stages. The algorithm for the first stage is shared in Algorithm 1, and for the second stage in Algorithm 2. A detailed explanation of these stages can be found in Section 3 of the actual paper.

### 9. Details on Evaluation Metrics

Below, we give a summary of the commonly used evaluation metrics.

**CLIP-T.** CLIP-T measures how well the generated image aligns with the textual prompt. It is computed as the cosine similarity between the CLIP embeddings of the input prompt and the generated image. We use the CLIP ViT-B/32 model [22] to obtain the embeddings. A higher CLIP-T score indicates stronger prompt adherence.

**CLIP-I.** CLIP-I evaluates image consistency by comparing the output generated with personalization against that generated without personalization. The cosine similarity between these two CLIP embeddings (again computed using the ViT-B/32 variant) reflects the model’s ability to inject identity-specific information without distorting the overall scene.

<sup>1</sup>Link: <https://github.com/ostris/ai-toolkit>

---

#### Algorithm 1: Stage-1 - Meta Training

---

**Input:**

- $buckets$ : the training dataset with the characters are grouped in buckets
- $r_1, r_2$ : Lora Down and Lora Mid output dimensions
- $N$ : number of characters per bucket
- $q_{bucket}$ : number of iterations with each bucket
- $q_{total}$ : number of total iterations
- $q_{warm-up}$ : iterations to only update LoM and LoU
- $bs$ : batch size

**Output:** Stage-1 weights of Meta-LoRA

$model \leftarrow \text{Meta-LoRA.initialize}(r_1, r_2, N)$ ;

$i_{curr} \leftarrow 0$ ;

**while**  $i_{curr} < q_{total}$  **do**

**for**  $bucket$  in  $buckets$  **do**

$data \leftarrow \text{Dataloader}(bucket, bs)$ ;

$i_{cb} \leftarrow 0$ ;

**for**  $batch$  in  $data$  and  $i_{cb} < q_{bucket}$  **do**

$loss \leftarrow model(batch)$ ;

**if**  $i_{cb} < q_{warm-up}$  **then**

                update-mid-and-up-layers( $loss$ );

**else**

                update-model( $loss$ );

$i_{cb} \leftarrow i_{cb} + 1$ ;

$i_{curr} \leftarrow i_{curr} + i_{cb}$ ;

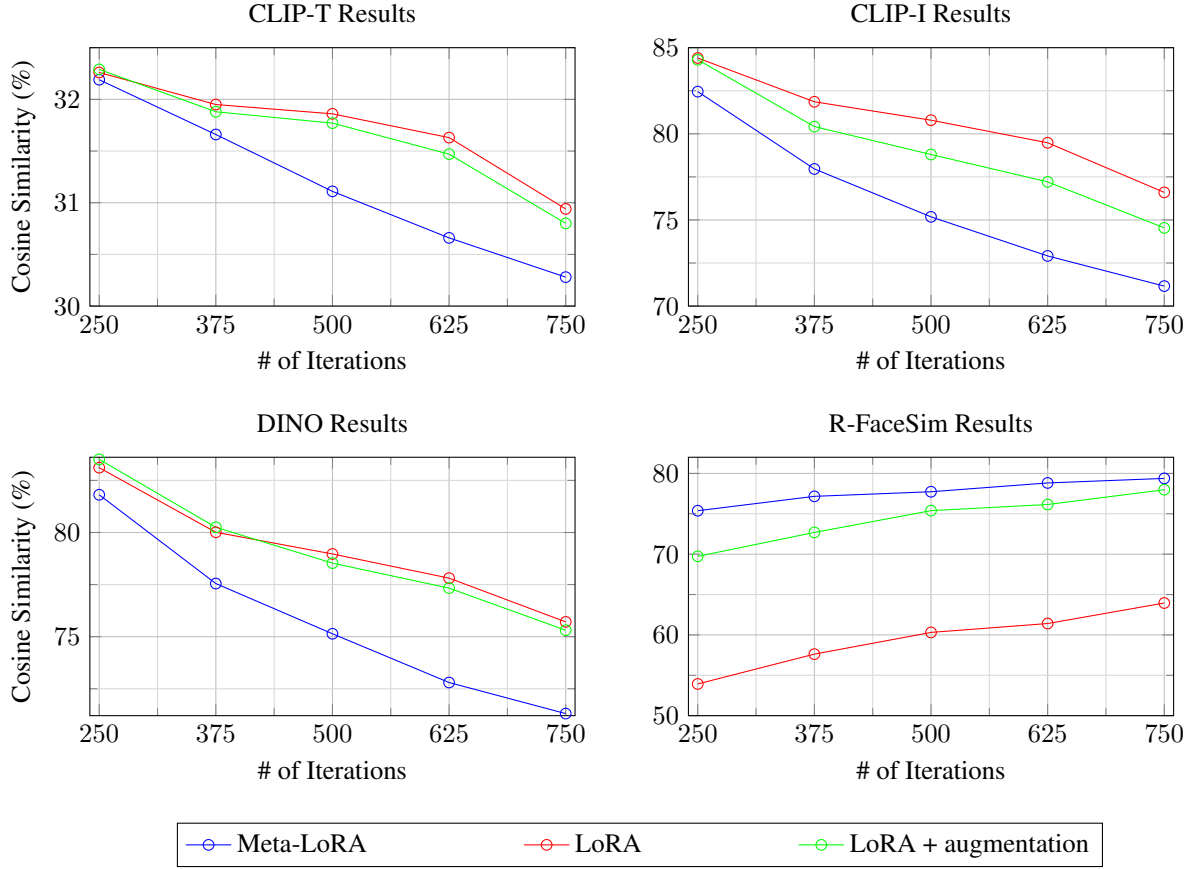
**return**  $model$

---

**DINO.** The DINO metric leverages the CLS token embedding from the DINO-pretrained ViT-S/16 (following [24] implementation) backbone to compute the cosine similarity between the generated personalized image and a base image. This metric provides a measure of global image similarity that complements the CLIP-based evaluations, capturing subtle visual details and overall subject fidelity.

**Conventional FaceSim details.** Conventional FaceSim metric is computed by extracting facial embeddings from the generated images using an Inception-ResNet [29] model pre-trained on VGGFace2 [2], followed by calculating the cosine similarity between these embeddings and those of the real subject. The a discussion on the shortcomings of the conventional FaceSim metric, and the proposed improved version is given in the experiments section of the main paper.

Figure 5. This figure visualizes the changes in the metric results of Meta-LoRA and default LoRA models with respect to number of iterations in the fine-tuning stage (stage-2 for MetaLoRA).




---

**Algorithm 2:** Stage-2 - Test-time ID Personalization

---

**Input:**

- $image_{person}$ : the single image of the person to learn
- $r_1, r_2$ : LoRA Down and Mid output dimensions
- $q_{st2}$ : Number of iterations
- $weights_{st1}$ : Stage-1 LoRA Down weights

**Output:**  $weights_{final}$ : Final Meta-LoRA Weights

```

model  $\leftarrow$  Meta-LoRA.initialize( $r_1, r_2, N$ );
load-down-weights(model,  $weights_{st1}$ );
dataset  $\leftarrow$  augment-and-create-data( $image_{person}$ );
for iter = 1 to  $q_{st2}$  do
    for item in dataset do
        loss  $\leftarrow$  model(batch);
        update-mid-and-up-layers(loss);
return model

```

---

## 10. LoRA and Meta-LoRA Training Curves

In this section, we analyze the performance dynamics of both LoRA and Meta-LoRA models during fine-tuning. Evaluations are conducted across the four primary metrics used in this paper—CLIP-T, CLIP-I, DINO, and R-FaceSim—at specific iteration points:  $q \in \{250, 375, 500, 625, 750\}$ . The results are presented in Figure 5.

As illustrated in the figure, Meta-LoRA exhibits a faster increase in R-FaceSim and a quicker decline in the other metrics compared to LoRA, indicating that it reaches a balanced state earlier, around 375 iterations. In contrast, the LoRA + augmentation model requires 625 iterations to achieve a similar equilibrium but with lower overall performance across all metrics. This demonstrates that Meta-LoRA not only accelerates learning but also outperforms standard LoRA in effectiveness.

To assess the impact of augmentation, we compare the performance of LoRA and LoRA + augmentation models. While both models follow a similar trend throughout training, the key distinction lies in their initial R-FaceSim performance at 250 iterations. The higher starting score of the



augmented model suggests that augmentation primarily enhances the learning process in the earliest training stages, leading to a more meaningful and stable convergence.

## 11. Qualitative Results

Figure 6 demonstrates extended comparison for a diverse set of inputs and reference images.

## 12. Baseline Model Details and Implementation Settings

**Model Variants and Base Diffusion Backbones.** We compare our Meta-LoRA personalization approach against several state-of-the-art subject-driven generation methods with publicly available implementations: InstantID [30], PhotoMaker [17], and PuLID [9]. Although each method’s GitHub demos recommend different diffusion backbones, to ensure a fair evaluation we run all SDXL-based methods under three popular variants:

- **SDXL-Base 1.0** (`stable-diffusion-xl-base-1.0`)
- **SDXL-RealVis 4.0** (`realvis-xl-4.0`)
- **SDXL-Lightning** (`sdxl-lightning`)

In contrast, our default LoRA and Meta-LoRA approaches are built on a FLUX-based model.

**Hardware and Data Types.** All SDXL-based experiments are conducted on a single NVIDIA RTX 3090 GPU with 24 GB VRAM, while the Flux-based PuLID inference (and our FLUX-based LoRA and Meta-LoRA) are performed on a single NVIDIA A6000 GPU with 48 GB VRAM (using CPU offload). In every case, we use `bf16` as the data type for inference.

**PuLID (SDXL and FLUX).** We adopt the newest PuLID Flux implementation (`FLUX_PuLID_v0.9.1`) from its public repository, which is claimed to improve upon the original paper’s version. For the SDXL-based PuLID model, we set `ID_scale=0.8` following the repository’s recommended configuration. For the Flux version, we set `id_weight=1.0`, `true_cfg=1.0`, `time_to_start_cfg=1`, `inference_steps=20`, `cfg=4.0`, and `max_sequence_length=128`, in accordance with the demo code.

**PhotoMaker.** We use `PhotoMakerV2`, which differs from the version evaluated in the PuLID paper [9] (where its performance was reported as poor, and claimed it is not even compatible with SDXL-Lightning). In our experiments, `PhotoMakerV2` yields substantially improved results—possibly owing to internal updates. Although `PhotoMakerV2` typically expects SDXL-RealVis4.0 as

its default backbone, we also evaluate it with SDXL-Lightning and SDXL-Base. To ensure compatibility with SDXL-Lightning (particularly for a 4-step inference), we set `time_spacing="trailing"` in the Euler scheduler configuration and adjust the `start_merge_step` parameter to 0 for SDXL-Lightning or 10 for SDXL-Base and SDXL-RealVis4.0. We further prepend the keyword “img” to each prompt (e.g., “man img ...”, “woman img ...”) to satisfy PhotoMaker’s trigger-word requirement.

**InstantID.** For InstantID, we consider two implementations:

1. The ComfyUI-based approach used in the PuLID paper [9], which exposes a “denoise” parameter in the `kSampler` node (with values between 0 and 1).
2. The original InstantID GitHub repository’s implementation.

In the ComfyUI setup, a denoise value in the range (0.8, 1.0] yields consistent sigma values ( $\{14.6146, 2.9183, 0.9324, 0.0292, 0.0000\}$  for a 4-step process) and markedly improves image quality for SDXL-Lightning. In the original repository, the time-step derivation departs from the standard SDXL pipeline, resulting in underdeveloped outputs. We therefore replace this part with the official SDXL pipeline (manually applying the aforementioned sigma values) to align the results with those from the ComfyUI version. For both implementations, we set `controlnet_conditioning_scale=0.8` and `ip_adapter_scale=0.8`. In spite of employing a robust negative prompt (see below) to counteract SDXL-FLUX artifacts, InstantID outputs tend to exhibit watermarks, a reflection of the training data characteristics. Following the InstantID GitHub recommendations, we generate images at  $1016 \times 1016$  and then resize them to  $1024 \times 1024$ , which reduces watermark occurrence.

**Prompting and Negative Prompts for SDXL Models.** All SDXL-based methods (InstantID, PhotoMaker, and PuLID-SDXL) share the following negative prompt:

*“flaws in the eyes, flaws in the face, flaws, lowres, non-HDRi, low quality, worst quality, artifacts noise, text, watermark, glitch, deformed, mutated, ugly, disfigured, hands, low resolution, partially rendered objects, deformed or partially rendered eyes, deformed, deformed eyeballs, cross-eyed, blurry”*

Flux-based methods (including PuLID-Flux, default LoRA, and Meta-LoRA) do not use any negative prompts, consistent with their default configurations.

**SDXL Inference Details.** We employ the Euler scheduler for all SDXL inferences:

Prompt	Input	FLUX.1-dev w/o ID	SDXL Lightning w/o ID	LoRA FLUX.1-dev	LoRA Augmented FLUX.1-dev	Meta-LoRA FLUX.1-dev (ours)	PuLiD FLUX.1-dev	PuLiD SDXL Lightning	InstantID SDXL Lightning	PhotoMaker SDXL Lightning
A man riding a bicycle under the Eiffel Tower, smiling at the camera										
A man as a medieval knight, wearing a shining armor, cinematic lighting										
A Pixar character of a man, expressive and exaggerated facial features										
A man sculpted out of marble, photorealistic, museum lighting										
A woman in a sunset backview, turning her head slightly towards the camera, warm glow on her face										
A mysterious woman witcher at night, glowing magical energy in her hands, looking directly at the viewer										
A woman as a futuristic android, half-human half-machine, glowing circuits on face										
A woman as an ink wash painting, traditional Asian art style, serene expression										

Figure 6. Qualitative comparisons for an extended list of baselines. See Section 4.5 for explanations.



Model	Base Model	Face Sim $\uparrow$	Robust Face Sim $\uparrow$	Relative Difference (%)
InstantID [30]	SD-XL [21]	80.17	71.33	-11.0%
	SD-XL Lightning [18]	82.91	74.77	-9.8%
	RealVisXL V4 [26]	81.11	73.10	-9.9%
PhotoMaker [17]	SD-XL	67.28	67.16	-0.2%
	SD-XL Lightning	66.67	63.02	-5.5%
	RealVisXL V4	68.94	68.57	-0.5%
PuLID [9]	SD-XL	78.84	71.06	-9.7%
	SD-XL Lightning	79.90	73.50	-8.0%
	RealVisXL V4	78.78	75.19	-4.6%
	FLUX.1-dev [15]	84.76	75.72	-10.7%
Rank-1 LoRA 375 Iters [10] + augmented inputs	FLUX.1-dev	60.60	57.62	-4.9%
	FLUX.1-dev	70.55	72.69	+3.0%
Rank-1 LoRA 625 Iters + augmented inputs	FLUX.1-dev	64.32	61.41	-4.2%
	FLUX.1-dev	76.77	76.15	-0.8%
Meta-LoRA	FLUX.1-dev	79.45	77.16	-2.9%

Table 2. Comparison of Robust Face Sim and Face Sim metrics, with percentage difference highlighted for significant drops.

- **SDXL-Lightning.** We adopt the 4-step `sdxl-lightning` checkpoint from ByteDance’s HuggingFace page, with `CFG-scale=1.2`, following recommendations from the PuLID paper [9].
- **SDXL-Base 1.0 and SDXL-RealVis 4.0.** We set `CFG-scale=5.0` and use 50 inference steps, in line with standard SDXL configurations.

**LoRA Baseline.** We also include a standard LoRA fine-tuning baseline [10] (implemented on a FLUX-based model) as a reference. A rank-1 LoRA is trained for each identity. Initially, we train for 375 iterations (to match Meta-LoRA’s Stage-2 steps), but observe that identity fidelity remains underfitted. We therefore extend training to 675 iterations and apply data augmentation strategies. Although these extended and augmented LoRAs show improved performance, our Meta-LoRA—with its meta-learned prior—converges faster and achieves higher identity fidelity in fewer steps.

**Justification for R-FaceSim.** As shown in Table 2, we observe a nontrivial gap between the conventional FaceSim scores and our proposed R-FaceSim scores. In particular, personalization approaches such as InstantID [30] and PuLID [9] often replicate the poses or gazes of the reference image, thereby artificially boosting FaceSim results. Meanwhile, PhotoMaker [17] is not as heavily affected by this phenomenon, as indicated by its relatively smaller discrepancy between the two metrics. Additionally, non-augmented LoRA baselines can overfit the position of the face in the generated image, further inflating their face similarity scores. This pose-copying and overfitting phenomenon conflates true identity fidelity with pose or spatial similarity, leading to overestimated accuracy in conventional FaceSim evaluations.

By contrast, R-FaceSim explicitly excludes the original reference image during evaluation and compares each generated output against multiple images of the same identity (captured under diverse conditions). This design ensures that high similarity scores genuinely reflect robust identity preservation rather than a mere replication of pose or gaze. Consequently, the observed differences in Table 2 (ranging up to 10% drop in some cases) highlight how pose-copying and overfitting can lead to inflated identity fidelity under conventional FaceSim. Our R-FaceSim metric thus offers a more stringent and realistic assessment of personalization performance, as it mitigates the bias introduced by reference-image reuse and captures fine-grained identity traits across varied visual contexts. We encourage future work to adopt this approach, especially when evaluating feed-forward or near-instant personalization methods that rely heavily on a single reference image.

**R-FaceSim.** The algorithm 3 computes the Robust Face Similarity Metric (R-FaceSim) by leveraging multiple images per identity, carefully chosen prompts, and a generative text-to-image model. For each identity, a single reference image is selected while the remaining images form the test set. The model is conditioned or fine-tuned using the reference image. For each prompt, the model generates an output image from which the face is cropped and its identity embedding extracted. This embedding is then compared via cosine similarity to the embeddings of faces from each test image. The mean similarity for a given prompt and identity is computed by averaging these cosine similarities. Finally, R-FaceSim is obtained by averaging the prompt-level similarities across all identities and prompts.

---

**Algorithm 3:** Robust Face Similarity Metric (R-FaceSim)

---

$I$     Set of identities with multiple images  
 $P$     Set of carefully chosen prompts  
**Input:**  $M$     Generative text-to-image model  
          $C$     Face cropper  
          $E$     Identity embedding extractor  
**Output:**  $R\text{-FaceSim}$ : Robust Face Similarity Score

```
for each  $i \in I$  do
   $ref \leftarrow \text{select\_one}(i)$ ;
   $T \leftarrow i \setminus \{ref\}$ ;
   $M \leftarrow \text{fine-tune/image-prompt}(M, ref)$ ;
  for each  $p \in P$  do
     $g \leftarrow M(p)$ ;
     $f_g \leftarrow C(g)$ ;
     $e_g \leftarrow E(f_g)$ ;
     $sumsim \leftarrow 0, count \leftarrow 0$ ;
    for each  $t \in T$  do
       $f_t \leftarrow C(t)$ ;
       $e_t \leftarrow E(f_t)$ ;
       $sim \leftarrow \text{cosine}(e_g, e_t)$ ;
       $sumsim \leftarrow sumsim + sim$ ;
       $count \leftarrow count + 1$ ;
     $S(i, p) \leftarrow \frac{sumsim}{count}$ ;
 $R\text{-FaceSim} \leftarrow \text{mean}\{S(i, p) : i \in I, p \in P\}$ ;
return  $R\text{-FaceSim}$ 
```

---

### 12.1. Evaluation Prompts

Table 3 and 4 include the prompts used in metric evaluations, used only with the Meta-PHD-FFHQ dataset. All metrics except R-FaceSim were calculated on these prompts.

The R-FaceSim metrics were calculated only on the Meta-PHD-UNSPLASH. Used for no other calculations. Designed specifically to provoke models to produce images where the person is facing the camera and no objects occluding their face.



Table 3. Meta-PHD-FFHQ Recontextualized Prompts

Prompt
A man in a firefighter uniform, standing in front of a firetruck, looking straight ahead.
A man in a spacesuit, floating in space with Earth in the background, face clearly visible.
A 90-year-old man with completely white hair, deep wrinkles covering his forehead, around his eyes, and mouth, looking at the viewer, well-lit portrait.
A man as a 1-year-old baby, joyful and playful, looking directly at the camera, soft lighting.
A man riding a bicycle under the Eiffel Tower, smiling at the camera.
A man playing a guitar in the forest, looking at the viewer, natural lighting.
A man working on a laptop in a modern office, facing forward with focused expression.
A man as a medieval knight, wearing a shining armor, cinematic lighting.
A man in a 1920s noir setting, wearing a fedora, moody lighting.
A man standing in the middle of a desert, wearing a long flowing scarf, looking at the camera as a sandstorm approaches.
A woman in a swimming pool, water reflecting on her face, looking straight ahead.
A woman in a sunset backview, turning her head slightly towards the camera, warm glow on her face.
A woman piloting a fighter jet, cockpit reflections visible, face clearly in focus.
A woman in New York, standing in Times Square, bright city lights illuminating her face.
A woman reading books in the library, facing forward, glasses on, scholarly expression.
A woman driving a car, cityscape in the background, focused expression, looking ahead.
A woman standing in the middle of a desert, wearing a long flowing scarf, looking at the camera as a sandstorm approaches.
A woman walking along a misty cobblestone street in an old European town, holding a vintage lantern, gazing into the distance.
A woman sitting on a rooftop at dusk, overlooking a glowing city skyline, sipping from a warm cup, smiling at the camera.
A woman in a 1920s noir setting, wearing a vintage dress, moody lighting.

Table 4. Meta-PHD-FFHQ Stylistic Prompts Examples

Prompt
A man as a cyberpunk character, neon lights reflecting on his face, highly detailed.
A man as an ink wash painting, traditional Asian art style, serene expression.
A man as a futuristic android, half-human half-machine, glowing circuits on face.
A man in an art nouveau portrait, elegant and highly stylized.
A Pixar character of a man, expressive and exaggerated facial features.
A man sculpted out of marble, photorealistic, museum lighting.
A pop-art style portrait of a man, bright colors and bold outlines.
A Funko pop figure of a man, oversized head, cartoonish features.
A pencil drawing of a man, highly detailed, face in full view.
A painting of a man in Van Gogh style, expressive brush strokes, looking at the viewer.
A woman as a cyberpunk character, neon lights reflecting on her face, highly detailed.
A woman as an ink wash painting, traditional Asian art style, serene expression.
A woman as a futuristic android, half-human half-machine, glowing circuits on face.
A woman in an art nouveau portrait, elegant and highly stylized.
A painting of a woman in Van Gogh style, expressive brush strokes, looking at the viewer.
A Pixar character of a woman, expressive and exaggerated facial features.
A woman sculpted out of marble, photorealistic, museum lighting.
A pop-art style portrait of a woman, bright colors and bold outlines.
A Funko pop figure of a woman, oversized head, cartoonish features.
A mysterious woman witcher at night, glowing magical energy in her hands, looking directly at the viewer.

Table 5. Meta-PHD-Unsplash Prompts - FaceSim

Prompt
A [man/woman] standing in a sunlit urban plaza, facing directly toward the camera with a fully visible, highly detailed face and direct eye contact.
A [man/woman] in a casual outfit, positioned in a blooming garden with soft natural light, [his/her] face clearly visible and [his/her] eyes meeting the camera.
A [man/woman] in a minimalist, modern outfit, set against a softly lit abstract background, with [his/her] face rendered in intricate detail and direct eye contact.
A [man/woman] in elegant attire, standing against a scenic landscape at sunrise, [his/her] face captured in sharp detail with a steady, direct gaze.
A [man/woman] in a relaxed, stylish ensemble, posed on a quiet beach at sunset, with a fully visible, richly detailed face and clear eye contact.
A [man/woman] in a fashionable outfit, placed in a vibrant urban art scene, with [his/her] face prominently visible, detailed, and looking straight at the camera.
A [man/woman] with a confident expression, standing in a serene park under bright daylight, [his/her] face rendered in high detail and engaging directly with the viewer.
A [man/woman] in a chic outfit, situated in a picturesque alleyway with soft ambient lighting, with [his/her] face clearly displayed in full detail and direct gaze.
A [man/woman] in a modern, casual look, standing in a contemporary indoor space with artistic lighting, [his/her] face fully visible and rendered with intricate detail as [he/she] looks at the camera.
A [man/woman] in a trendy outfit, positioned in a lively outdoor market where natural light highlights [his/her] features, [his/her] face completely unobstructed and detailed, with direct eye contact.